

SUPPORTING INFORMATION

Field-Induced Single-Ion Magnet Behavior in Two New Cobalt(II) Coordination Polymers with 2,4,6-Tris(4-pyridyl)-1,3,5-triazine

Dong Shao¹, Le Shi¹, Hai-Yan Wei^{2,*} and Xin-Yi Wang^{1,*}

¹ State Key Laboratory of Coordination Chemistry, Collaborative Innovation Center of Advanced Microstructures, School of Chemistry and Chemical Engineering, Nanjing University, Nanjing 210023, China; shaodong1130@163.com (D.S.); leshiyun1994@163.com (L.S.)

² Jiangsu Key Laboratory of Biofunctional Materials, School of Chemistry and Materials Science, Nanjing Normal University, Nanjing 210023, China

* Correspondence: weihaiyan@njnu.edu.cn (H.-Y.W.), wangxy66@nju.edu.cn (X.-Y.W.); Fax: +86-25-89682309 (X.-Y.W.)

Table of Contents

Table S1. Data Collection and Structure Refinement Parameters for 1 and 2	2
Table S2. Selected bond lengths (Å) and bond angles (°) for compounds 1 and 2	3
Figure S1. The asymmetric unit of 1	4
Figure S2. The packing structure of 1	4
Figure S3. The asymmetric unit of 2	5
Figure S4. The packing structure of 2	5
Figure S5. Frequency dependence of ac magnetic susceptibilities for 1 (left) and 2 (right) measured at 2 K in various applied fields from 0 to 4000 Oe	6
Figure S6. Cole-Cole plots for 1 (up) and 2 (down) at 2 K under various applied dc fields. The solid lines represent the best fits of the experimental results with the generalized Debye model	6
Figure S7. Frequency dependence of the in-phase (χ'') and out-of-phase (χ''') parts of the ac magnetic susceptibilities for 1 and 2 collected under 1200 and 800 Oe dc fields, respectively.	7
Table S3. Compilation of 1D, 2D, and 3D Co ^{II} Single-Ion Magnets.	7
Table S4. Relaxation fitting parameters at different temperatures under 1200 Oe from the least-square fitting of the Cole-Cole plots of complex 1 according to the generalized Debye model	8
Table S5. Relaxation fitting parameters at different temperatures under 800 Oe from the least-square fitting of the Cole-Cole plots of complex 2 according to the generalized Debye model	9
Figure S8. Thermal gravimetric analyses (TGA) for 1 and 2	10

Figure S9. Experimental and calculated PXRD patterns for **1** and **2** 10

Table S1. Data Collection and Structure Refinement Parameters for **1** and **2**.

Complex	1	2
Formula	C ₁₆ H ₃₀ CoN ₄ O ₁₂	C ₂₀ H ₂₁ CoN ₆ O ₆
Mr. / g mol ⁻¹	529.37	500.36
T, K	150	150
crystal system	Rhombohedral	Monoclinic
space group	<i>R</i> $\bar{3}m$	<i>C2/c</i>
<i>a</i> [Å]	26.6990(7)	24.6003
<i>b</i> [Å]	26.6990(7)	10.9748
<i>c</i> , [Å]	9.1870(5)	7.3936
α [deg]	90	90
β [deg]	90	91.229(8)
γ [deg]	120	90
<i>V</i> [Å ³]	5671.5(4)	1995.7(9)
<i>Z</i>	9	4
ρ_{calcd} [g cm ⁻³]	1.395	0.915
<i>F</i> (000)	2493	1032
<i>R</i> _{int}	0.0384	0.0713
<i>T</i> _{man} , <i>T</i> _{min}	0.9096, 0.7970	0.8749, 0.6943
Data / restraints / parameters	2534 / 0 / 87	3319 / 0 / 153
<i>R</i> 1, <i>wR</i> 2 [$I \geq 2\sigma(I)$] ^[a]	0.0326, 0.0945	0.0524, 0.1374
<i>R</i> 1, <i>wR</i> 2 (all data) ^[a]	0.0366, 0.0969	0.0638, 0.1441
GOF	1.102	1.053
Max/min / e [Å ⁻³]	0.520, -0.679	0.654, -0.725
^a $R_1 = \sum F_O - F_C / \sum F_O $ ^b $wR_2 = \{\sum [w(F_O^2 - F_C^2)2] / \sum [w(F_O^2)^2]\}^{1/2}$		

Table S2. Selected bond lengths (\AA) and bond angles ($^\circ$) for compounds **1** and **2**.

	1		2
Co(1)-O(1)	2.071(1)	Co(1)-O(1)	2.1268(1)
Co(1)-O(1)#1	2.071(1)	Co(1)-O(1)#1	2.1268(1)
Co(1)-O(1) #2	2.071(3)	Co(1)-O(2)	2.0556(1)
Co(1)-O(1)#3	2.071(3)	Co(1)-O(2)#1	2.0556(1)
Co(1)-N(1)	2.144(4)	Co(1)-N(1)	2.1765(1)
Co(1)-N(1)#3	2.144(4)	Co(1)-N(1)#1	2.1765(1)
Co-X _{average} (X = N, O)	2.095(5)	Co-X _{average} (X = N, O)	2.119(6)
O(1)#1-Co(1)-O(1)#2	180	O(1)#1-Co(1)-O(1)	180.0
O(1)#1-Co(1)-O(1)	90.36(5)	O(2)-Co(1)-O(1)#1	84.10(6)
O(1)#2-Co(1)-O(1)	89.64(5)	O(2)#1-Co(1)-O(1)#1	95.90(6)
O(1)#1-Co(1)-O(1)#3	89.64(5)	O(2)#1-Co(1)-O(1)	84.10(6)
O(1)-Co(1)-O(1)#3	180.00(4)	O(2)-Co(1)-N(1)	91.49(6)
O(1)-Co(1)-N(1)#3	93.37(4)	O(2)#1-Co(1)-N(1)	88.51(6)
O(1)#1-Co(1)-N(1)#3	93.37(4)	O(1)#1-Co(1)-N(1)	87.43(6)
O(1)#1-Co(1)-N(1)	86.63(4)	O(1)-Co(1)-N(1)	92.57(6)
Symmetry transformations used to generate equivalent atoms: #1 -x+y+1,y,z; #2 x-y,-y,-z+2 #3 -x+1,-y,-z+2 for 1 ; #1 -x+1/2,-y+3/2,-z, #2 -x,y,-z+1/2 for 2 .			

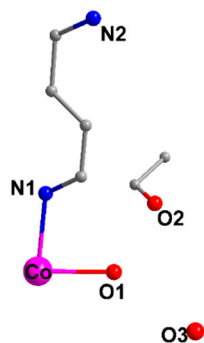


Figure S1. The asymmetric unit of **1**.

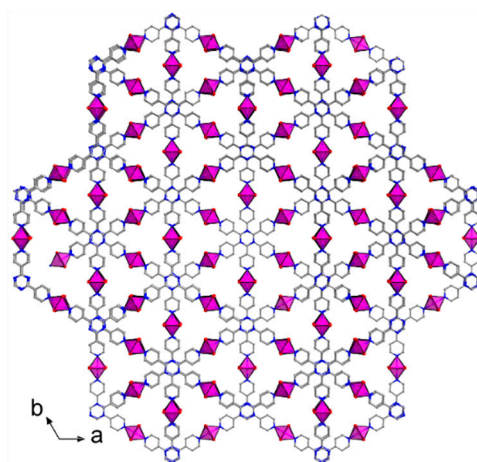


Figure S2. The packing structure of **1**.

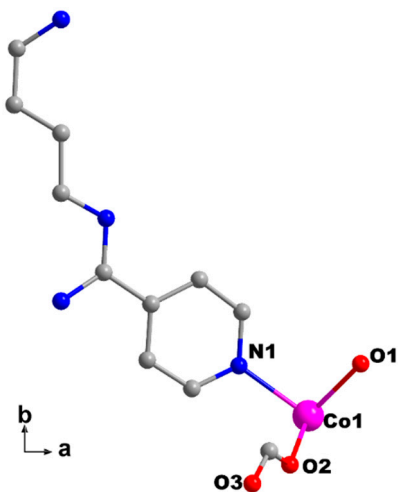


Figure S3. The asymmetric unit of 2.

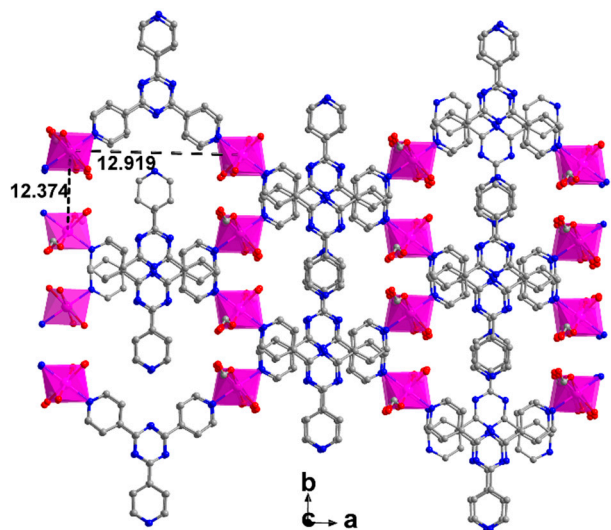


Figure S4. The packing structure of 2.

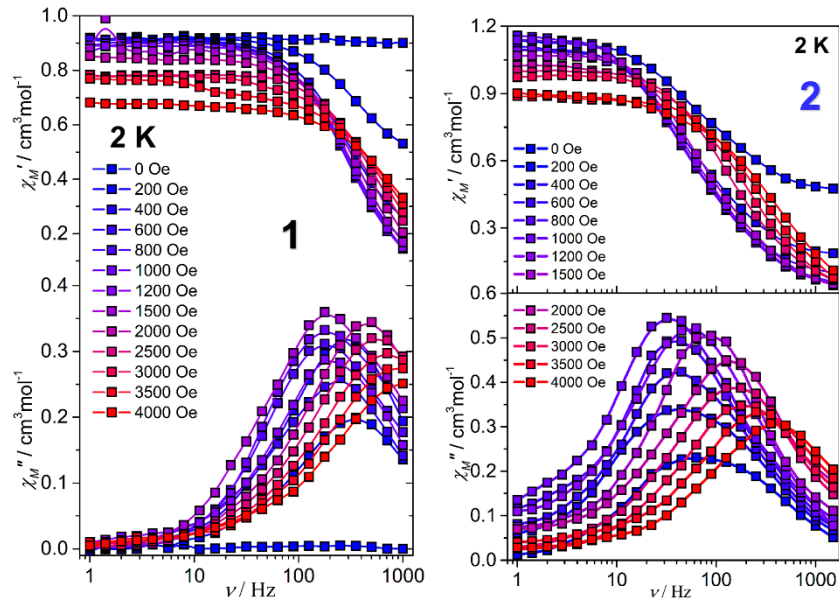


Figure S5. Frequency dependence of ac magnetic susceptibilities for **1** (left) and **2** (right) measured at 2 K in various applied fields from 0 to 4000 Oe.

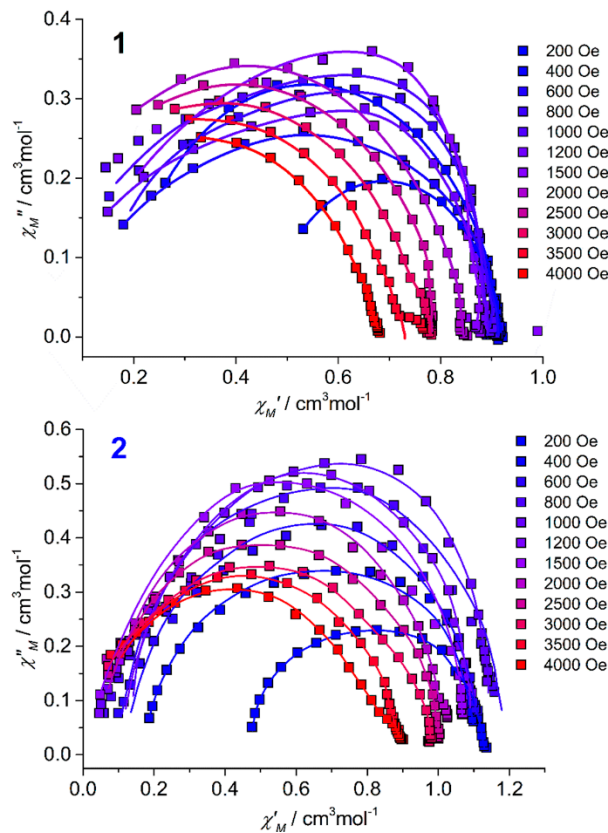


Figure S6. Cole-Cole plots for **1** (up) and **2** (down) at 2 K under various applied dc fields. The solid lines represent the best fits of the experimental results with the generalized Debye model.

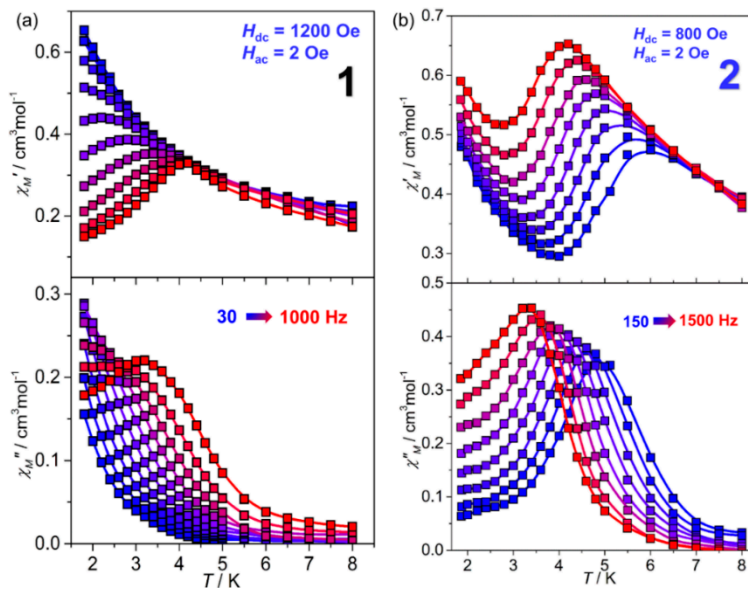


Figure S7. Frequency dependence of the in-phase (χ'') and out-of-phase (χ''') parts of the ac magnetic susceptibilities for **1** and **2** collected under 1200 and 800 Oe dc fields, respectively.

Table S3. Compilation of 1D, 2D, and 3D Co^{II} Single-Ion Magnets.

Compound	dimensionality	D/cm^{-1}	$U_{\text{eff}}/\text{K} (\text{H/Oe})$	Ref.
[Co(btm) ₂ (SCN) ₂ ·H ₂ O] _n	1D	93.9	45.5	S1
{[Co(bpeb) ₂ (NCS) ₂]·7DCB} _n	2D	64.9	131.3	S3
{[Co(bpeb) ₂ (NCS) ₂]·4TAN} _n	2D	67.1	137.8	S3
{[Co(bpeb) ₂ (NCS) ₂]·6TOL} _n	2D	84.4	169.7	S3
{[Co(bpeb) ₂ (NCS) ₂]·8PYR} _n	2D	70.3	143.7	S3
[Co(dca) ₂ (bim) ₄] _n	2D	69.6	7.8-11.1	S4
[Co(dca) ₂ (bim) ₂] _n	2D	74.3	6.5-13.3	S4
[Co(dca) ₂ (bmim) ₂] _n	2D	75.8	16.5-22.2	S4
{[Co(3,3'-Hbpt) ₂ (SCN) ₂]·2H ₂ O} _n	2D	70.1	105.1	S5
[Co(L) ₂ (SCN) ₂ ·2(CH ₃ CN)·2(dmf)] _n	2D	41.6	36.9	S6
[Co(dca) ₂ (atz) ₂] _n	2D	/	7.3	S7
{[Co(bmzbc) ₂]·2DMF} _n	2D	62.6	11.8	S8
[Co(ppad) ₂] _n	2D	76	16.3	S9
[Co(bmzbc) ₂ (Hbmzbc)] _n	2D	/	31.3	S10
{[(Co(NCS) ₂ (H ₂ O) _{0.65} (MeOH) _{0.35}) ₃ (k ³ -)} _n	2D	> 90	/	S11
[Co(bmzbc) ₂ (1,2-etdio)] _n	3D	/	16.8	S10
{[(Co(NCS) ₂) ₃ (k ³ -)} _n	3D	> 130	7	S11

- S1. Zhu, Y.-Y.; Zhu, M.-S.; Yin, T.-T.; Meng, Y.-S.; Wu, Z.-Q.; Zhang, Y.-Q.; Gao, S. *Inorg. Chem.* **2015**, *54*, 3716-3718.
- S2. Ma, R.-R.; Chen, Z.-W.; Cao, F.; Wang, S.; Huang, X.-Q.; Li, Y.-W.; Lu, J.; Lia, D.-C.; Dou, J.-N. *Dalton Trans.* **2017**, *46*, 2137-2145.
- S3. Vallejo, J.; Fortea-Perez, F. R.; Pardo, E.; Benmansour, S.; Castro, I.; Krzystek, J.; Armentano, D.; Cano, J. *Chem. Sci.* **2016**, *7*, 2286-2293.
- S4. Świtlicka-Olszewska, A.; Palion-Gazda, J.; Klemens, T.; Machura, B.; Vallejo, J.; Cano, J.; Lloret, F.; Julve, M. *Dalton Trans.* **2016**, *45*, 10181-10193.
- S5. Sun, L.; Zhang, S.; Chen, S.-P.; Yin, B.; Sun, Y.-C.; Wang, Z.-X.; Ouyang, Z.-W.; Ren, J.-J.; Wang, W.-Y.; Wei, Q.; Xie, G.; Gao, S.-L. *J. Mater. Chem. C* **2016**, *4*, 7798-7808.
- S6. Mondal, A. K.; Khatua, S.; Tomar, K.; Konar, S. *Eur. J. Inorg. Chem.* **2016**, 3545-3552.
- S7. Palion-Gazda, J.; Klemens, T.; Machura, B.; Vallejo, J.; Lloret, F.; Julve, M. *Dalton Trans.* **2015**, *44*, 5989.
- S8. Wang, Y.-L.; Chen, L.; Liu, C.-M.; Du, Z.-Y.; Chen, L.-L.; Liu, Q.-Y. *Inorg. Chem.* **2015**, *54*, 11362-11368.
- S9. Liu, X.-Y.; Sun, L.; Zhou, H.-L.; Cen, P.-P.; Jin, X.-Y.; Xie, G.; Chen, S.-P.; Hu, Q.-L. *Inorg. Chem.* **2015**, *54*, 8884-8886.
- S10. Wang, Y.-L.; Chen, L.; Liu, C.-M.; Du, Z.-Y.; Chen, L.-L.; Liu, Q.-Y. *Dalton Trans.* **2016**, *45*, 7768-7775.
- S11. Brunet, G.; Safin, D. A.; Jover, J.; Ruiz, E.; Murugesu, M. *J. Mater. Chem. C* **2017**, *5*, 835-841.

Table S4. Relaxation fitting parameters at different temperatures under 1200 Oe from the least-square fitting of the Cole-Cole plots of complex **1** according to the generalized Debye model.

T / K	$\chi_S / \text{cm}^3\text{mol}^{-1}\text{K}$	$\chi_T / \text{cm}^3\text{mol}^{-1}\text{K}$	τ / s	α
1.8	0.05151	0.69885	7.9E-4	0.10735
2.0	0.05226	0.64185	6.6E-4	0.11401
2.2	0.06089	0.59262	5.5E-4	0.09004
2.4	0.07	0.54952	4.6E-4	0.05927
2.6	0.09	0.51018	3.8E-4	0.05141
2.8	0.10091	0.47467	3.4E-4	0.01545
3.0	0.12	0.45592	3E-4	0
3.2	0.14152	0.42847	2.6E-4	0.00423
3.4	0.16021	0.412	2.4E-4	0
3.6	0.1903	0.3905	2.3E-4	0.00146
3.8	0.21014	0.37603	2.1E-4	0.00177
4.0	0.22154	0.35938	1.9E-4	0.00108

Table S5. Relaxation fitting parameters at different temperatures under 800 Oe from the least-square fitting of the Cole-Cole plots of complex **2** according to the generalized Debye model.

T / K	$\chi_S / \text{cm}^3\text{mol}^{-1}\text{K}$	$\chi_T / \text{cm}^3\text{mol}^{-1}\text{K}$	τ / s	α
1.8	0.38008	1.36233	0.0015	0.23355
2.0	0.36036	1.29158	0.00145	0.22283
2.2	0.32036	1.20144	0.0014	0.20807
2.4	0.29022	1.13877	0.00134	0.19915
2.6	0.27072	1.08018	0.00125	0.19155
2.8	0.25	1.02618	0.00115	0.16948
3.0	0.26061	0.94161	0.00105	0.13104
3.2	0.22086	0.91512	9.4E-4	0.11588
3.4	0.21064	0.86303	8.4E-4	0.07239
3.6	0.2005	0.82031	7.3E-4	0.04657
3.8	0.2	0.78401	5.9E-4	0.02708
4.0	0.19062	0.75113	5.0E-4	0.01371
4.2	0.2004	0.72098	4.4E-4	0.00644
4.4	0.21043	0.69208	3.8E-4	0.00336
4.6	0.24003	0.66384	3.0E-4	0.00173
4.8	0.27011	0.64144	2.6E-4	7.831E-4
5.0	0.30016	0.61714	2.3E-4	3.44E-4

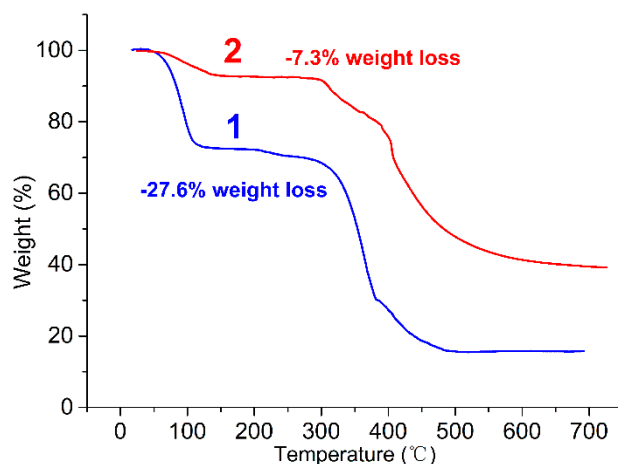


Figure S8. Thermal gravimetric analyses (TGA) for **1** and **2**.

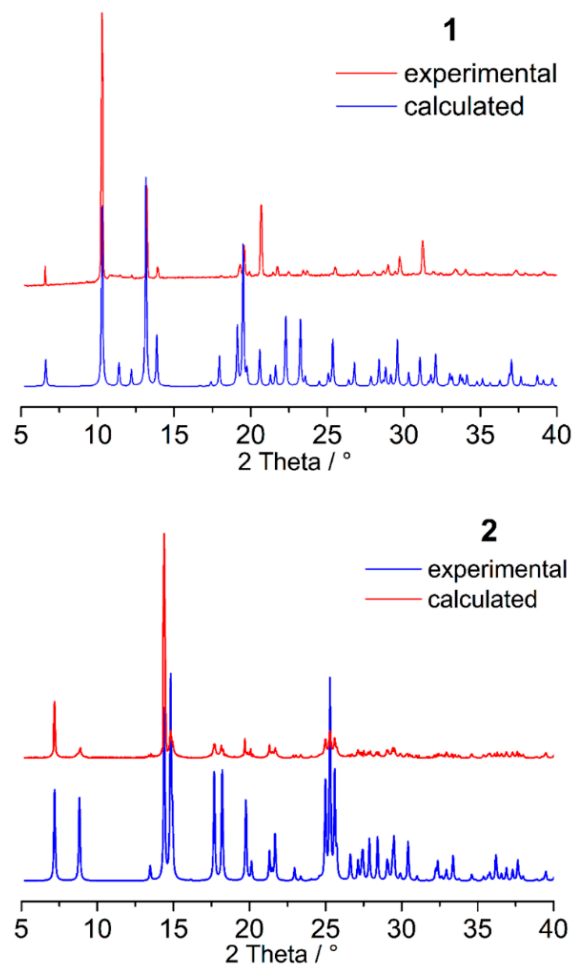


Figure S9. Experimental and calculated PXRD patterns for **1** and **2**.